

NUMERICAL STUDY TO PREDICT PROPERTIES OF WAXY CRUDE OIL UNDER DYNAMIC COOLING

Goh K. Hwa¹, Girma Tadesse Chala^{2*}

¹INTI International University, Negeri Sembilan, Malaysia

²International College of Engineering and Management, Muscat, Oman

*E-mail: girma@icem.edu.om

ABSTRACT

In this paper, a parametric study was conducted via ANSYS-Fluent workbench to predict the properties of waxy crude oil subjected to dynamic cooling. Different case studies were conducted to validate the numerical study, and prediction of temperature for pipelines of up to 100 m length was made. It was observed that the percentage difference between the experimental and simulation results was below 20%. The temperature drop was smaller with a higher flow rate, with the temperature dropping from 350K to 338K in an uninsulated pipe of 100 m length. The temperature drop for lower flow rate could be considered significant to reach wax appearance temperature during dynamic cooling. This study would be a supporting step to involve simulation in predicting the properties of waxy crude oil in different pipe sizes.

Keywords: Waxy crude oil, dynamic cooling, ANSYS-Fluent, parametric study

INTRODUCTION

In the oil industry, the transportation of waxy crude oil has primarily been challenged by the high amount of waxes in the crude oil [1]-[3]. Waxy crude oil consists of wax (paraffin) that crystallises below a specific temperature [4]-[6]. The wax content tends to vary according to the API and oil production area, which indicates that the rheological properties of the waxy crude oil are different for different waxy crude oils [7]-[8]. When waxy crude oil is under a thermal gradient environment such as the seabed at offshore fields, a significant amount of heat loss could occur, decreasing the temperature of waxy crude oil proportionally to the travelling distances and affecting the oil viscosity [9]. This eventually leads to poor oil transportation efficiency and, finally, pipeline blockage [10]. The blockages require restart operation, such as applying high pressure to resume the flow of waxy crude oil in pipelines [11]. Flow assurance of waxy crude oil production, especially in high paraffinic oil fields, faces a significant challenge about waxy

crude oil transportation in longer pipelines under seabed [12]-[14]. This condition may yield a flow breakdown that would have significant problems while resuming the steady flow again. This finally reduces the production as there would be inactive operation during shutdown that eventually influences the production costs [15].

The waxy crude oil's shear-dependent and temperature-dependent nature would vary the viscosity and yield stress in some conditions [16]-[18]. While the variation of viscosity would initiate the thixotropic behavior of waxy crude oil, many researchers developed numerical models by considering this behavior in their models to simulate and estimate the optimum pressure for flow restart of waxy crude oil [19]-[21]. The most convenient method used by the industry for cost-effective transportation of waxy crude oil is early prevention. Firmansyah et al. [22] stated that wax removal could be performed by heat treatment with the use of an external coil for inductive heating. Another method is preheating treatment with heated

crude oil to allow the compressible gel-crude oil to resume. It was recommended to maintain the crude oil at a threshold temperature margin which is 5°C higher than the pour point temperature, so that the crude oil would not solidify at a rapid pace. Fleyfel et al. [23] reports also showed that coating the pipeline with insulation didn't show satisfying results.

Elam et al. [24] experimented that the thermal conductivity of the given crude oil can be measured accurately using the hot wire method, with a solvent mixture of water-glycerol. The correlation in predicting the binary mixture of thermal conductivity showed promising results in conjunction with the realistic physical value obtained from the aromatic and paraffinic division. Huang et al. [25] investigated mass and heat transfer for the flow type of laminar and turbulence to develop a mathematical model in forecasting the thickness and fractions of wax accumulations. The outcome by involving the kinetic model of wax precipitation in oil showed promising results in predicting the wax deposition in both pilot-scale and lab-scale experiments.

The core annular method is a valuable method used in the industry where water film flows around the oil core to transport heavy crude oil [26]. The usage of water also acts as a lubricant to smoothen transportation. The disadvantage of using this method is that oil tends to stick to the wall while transporting in the pipeline. This may block and restrict the flow in a certain period, requiring a higher restart pressure after a maintenance or shutdown period. Drag Reducing Agent (DRA) for transporting waxy crude oil reduces fanning factor and pressure drops, along with reducing the energy required, which finally increases transportation capacities. However, based on Hassanean et al. [27], with a higher concentration of DRA, the molecular weight increases leading to high fluid viscosity. To ease the restarting of gelled waxy crude oil, one of the recently suggested methods is injecting non-reacting gas in several selected points before or during the shutdown period. The work of Sulaiman et al. [28] showed a lower restart pressure with nitrogen injection as a result of increased slippage effects, alternately saving costs. Moreover, nitrogen gas production is much more economical and has lower installation complexity than other non-reacting gases.

Although the deposition of the wax during dynamic cooling would be much lower than that of statically cooled pipelines, it was assumed that there would be a higher temperature drop in waxy crude oil subjected to dynamic cooling with a potential of gel formation [29]-[31]. Therefore, this study's objective was to predict the properties of waxy crude oil in longer pipelines subjected to dynamic cooling. This would help predict temperatures in longer pipelines to indicate the magnitude change, leading to wax precipitation.

MATERIALS AND METHODS

Simulation Techniques

A parametric study was conducted using the ANSYS-FLUENT workbench. Initially, the model was designed by the design modeller. In the experiment conducted, the initial temperature was 80°C, and the surrounding temperature was between 17°C and 20°C. The simulated pipe was an acrylic pipe with a diameter of 30 mm and a length of 1.2 m. The amount of mesh sizing was set at a medium rate to obtain optimum analysis period and result. As there are no similar materials in the ANSYS database that can categorise the waxy crude oil and acrylic, user-defined data for properties of waxy crude oil was inputted into the FLUENT database. Table 1 shows the properties of waxy crude oil used in this study.

Table 1 Properties of waxy crude oil

Density, $\rho \left(\frac{kg}{m^3} \right)$	850
Specific Heat, $C_p \left(\frac{J}{kg \cdot K} \right)$	3000
Thermal Conductivity $\left(\frac{W}{m \cdot K} \right)$	0.6
Dynamic Viscosity (Pa-s)	0.002

Simulation Method

ANSYS-Fluent workbench was used to simulate the flow of waxy crude oil subjected to dynamic cooling.

In solving the analysis, the equations of conservation of mass and momentum were used. The conservation of energy equation was also applied as the scenario considered involves the transfer of heat.

The continuity equation was given as:

$$\frac{\partial \rho}{\partial t} + \nabla \cdot (\rho \vec{v}) = S_m \quad (1)$$

As for the 2D axisymmetric geometry model, the continuity equation was stated as:

$$\frac{\partial \rho}{\partial t} + \frac{\partial}{\partial x}(\rho v_x) + \frac{\partial}{\partial r}(\rho v_r) + \frac{\rho v_r}{r} = S_m \quad (2)$$

where the v_x is the axial pace, v_r is the radial pace, x is the axial correlation, while r is the radial correlation.

The conservation of momentum is given as follows :

$$\frac{\partial \rho}{\partial t}(\rho \vec{v}) + \nabla \cdot (\rho \vec{v} \vec{v}) = -\nabla p + \nabla \cdot (\bar{\tau}) + \rho \vec{g} + \vec{F} \quad (3)$$

where static pressure represents as p , the $\bar{\tau}$ represents stress tensor, and $\rho \vec{g}$ and \vec{F} serve as the gravitational body force and external body force respectively. From Equation 3, the stress tenor $\bar{\tau}$, also known as the second-order tensor t , consists of nine components that define the stress condition at a point inside a material in the configuration, deform, and placement state. Thus, it can be written as,

$$\bar{\tau} = \mu \left[(\nabla \vec{v} + \nabla \vec{v}^T) - \frac{2}{3} \nabla \vec{v} I \right] \quad (4)$$

where μ is the molecular viscosity, the tensor unit is represented as I .

The axial and radial momentum for the conservation of equation for the 2D axisymmetric geometry can be defined as,

$$\begin{aligned} \frac{\partial}{\partial t}(\rho v_x) + \frac{1}{r} \frac{\partial}{\partial x}(r \rho v_x v_x) + \frac{1}{r} \frac{\partial}{\partial r}(r \rho v_r v_x) = \\ -\frac{\partial p}{\partial x} + \frac{1}{r} \frac{\partial}{\partial r} \left[r \mu \left(2 \frac{\partial v_x}{\partial x} - \frac{\partial v_r}{\partial x} (\nabla \cdot \vec{v}) \right) \right] + \\ \frac{1}{r} \frac{\partial}{\partial r} \left[r \mu \left(\frac{\partial v_x}{\partial r} + \frac{\partial v_r}{\partial x} \right) \right] + F_x \end{aligned} \quad (5)$$

$$\begin{aligned} \frac{\partial}{\partial t}(\rho v_r) + \frac{1}{r} \frac{\partial}{\partial x}(r \rho v_x v_r) + \frac{1}{r} \frac{\partial}{\partial r}(r \rho v_r v_r) = \\ -\frac{\partial p}{\partial r} + \frac{1}{r} \frac{\partial}{\partial r} \left[r \mu \left(2 \frac{\partial v_r}{\partial r} - \frac{2}{3} (\nabla \cdot \vec{v}) \right) \right] + \\ \frac{1}{r} \frac{\partial}{\partial x} \left[r \mu \left(\frac{\partial v_r}{\partial x} + \frac{\partial v_x}{\partial r} \right) \right] - 2 \mu \frac{v_r}{r^2} + \frac{2}{3} \frac{\mu}{r} (\nabla \cdot \vec{v}) \\ + \rho \frac{v_z^2}{r} + F_r \end{aligned} \quad (6)$$

The velocity vector was calculated by,

$$\nabla \cdot \vec{v} = \frac{\partial v_x}{\partial x} + \frac{\partial v_r}{\partial r} + \frac{v_r}{r} \quad (7)$$

And the swirl velocity is denoted as v_r .

Heat transfer was involved in predicting the properties of waxy crude oil as the pipelines lost heat toward the surrounding weather. In ANSYS FLUENT, there were several energy equations involved in the analysis. The energy equation is equated as,

$$\begin{aligned} \frac{\partial \rho}{\partial t}(\rho E) + \nabla \cdot (\vec{v}(\rho E + p)) = \nabla \cdot \left(k_{eff} - \sum_j h_j \vec{J}_j + \right. \\ \left. (\bar{\tau}_{eff} \cdot \vec{v}) \right) + S_h \end{aligned} \quad (8)$$

where k_{eff} represents effective conductivity and diffusion flux of species stated as \vec{J}_j . S_h represents the heat of any chemical reaction and any other volumetric heat sources defined.

RESULTS AND DISCUSSION

Figure 1 shows the 3D plot for inlet and outlet pressures for the flow rate of 20 L/min. The results simulate that of Riberio et al. [32]. The case was forecasted with the condition of constant flow rate with the outcome of change in pressure. The wax particle accumulates along the line and would eventually attach to the wall. The inlet pressure shows similar trends where the pressure increases and starts to reduce after the turning point. Figure 2 shows the patterns for the 15 L/min flow rate. The flow pattern is similar to the one predicted by Riberio's research, but many experiment points show deviation compared to the 20 L/min flow chart. The pattern of scattering seems to be easy to grasp in this case. The pattern

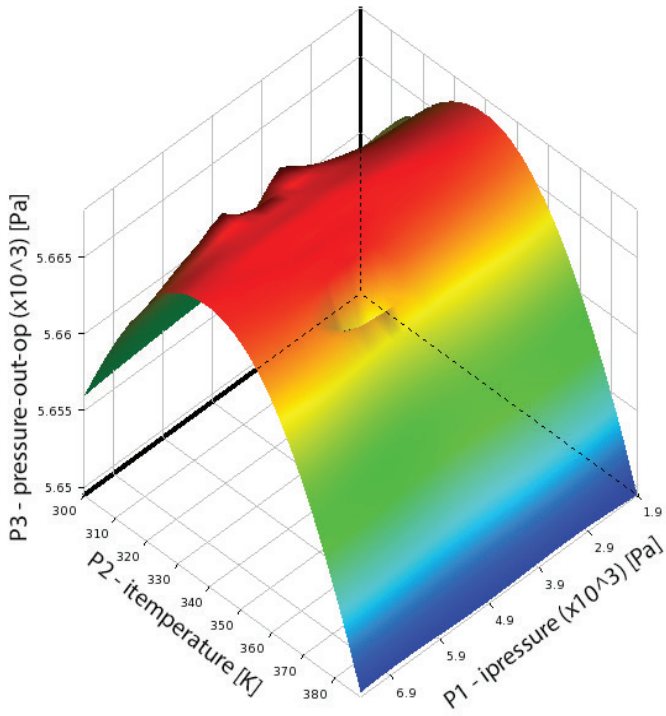


Figure 1 3D plot for inlet input against pressure outlet for the flow rate of 20 L/min

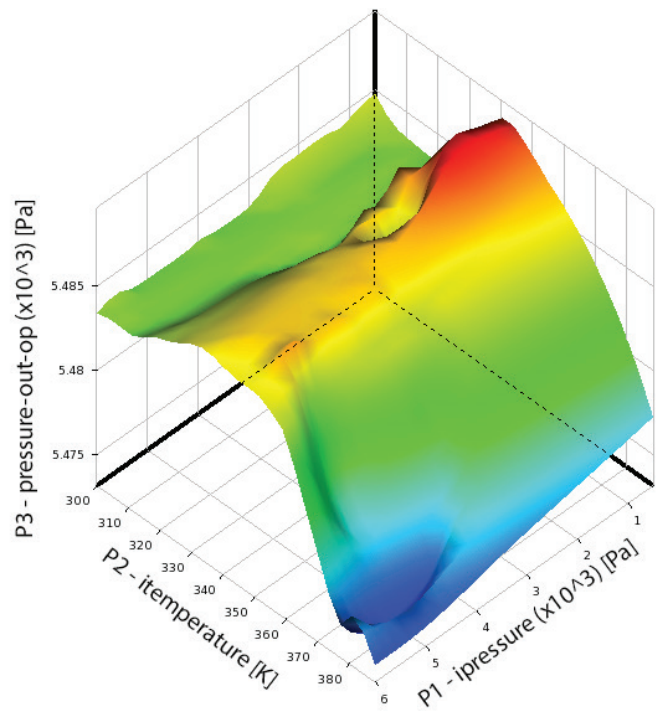


Figure 2 3D plot for inlet input against pressure outlet for 15 L/min flow

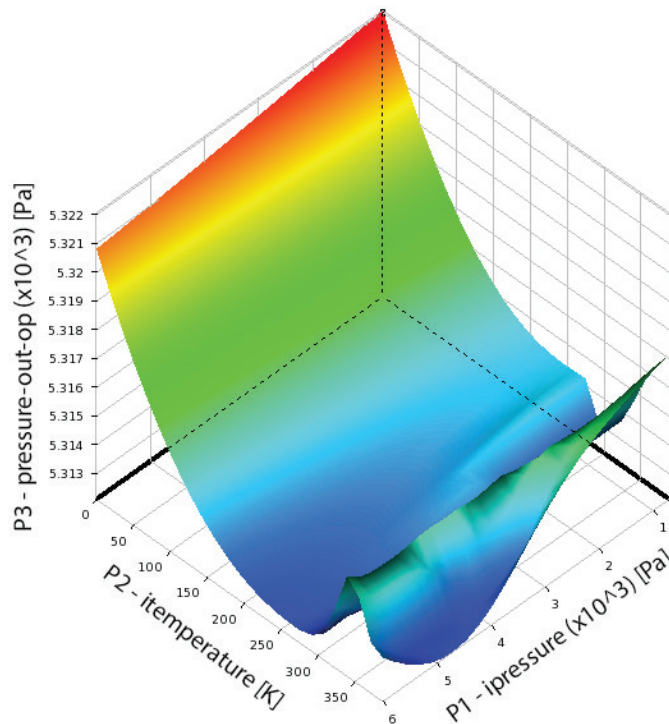


Figure 3 3D plot for inlet input against pressure outlet for 10 L/min flow

for the volume flow rate of 10 L/min flow is shown in Figure 3. The crude oil flow properties deviate when it reaches lower than 303K.

A higher flow rate exhibits the smoothest transportation and the slightest pressure fluctuation compared to the other flow rates. Temperature drop along the pipeline was showing similar trends. The temperature dropped along the pipeline as the transfer of heat constantly occurred between the pipe and surrounding. In the non-Newtonian region, ANSYS simulation may not fully exhibit the crude oil phase transition characteristics. Thus the experimental result must act as the initial comparison before simulation outcomes are used in future analysis.

Model Validation

The simulated output data are compared with the experimental data for validation purposes. The comparison of temperature is made in terms of degree celsius for more accessible analysis at the outlet of the acrylic pipe. The percentages of difference between the experimental and simulated results were calculated. Figure 4 compares experimental and simulation results for 20 L/min. The difference between the experimental and simulation results is at an average of 2.6%. Besides, the simulation data also followed the trend of the experimental data where there is a spike at the trial count of 82, showing the reliability of simulated results. When the temperature drops to around 46°C, the difference

started to increase due to phase changes. Hence, the simulation can no longer be compared in the solid phase as that involves multiphase flow in the Non-Newtonian region.

Figure 5 shows the percentage difference between experimental and simulation results for the 15 L/min flow rate. The percentage difference between the experiments and simulation was 1.7% which is the lowest among the others. The percentage difference between experimental and simulation results for 10 L/min is shown in Figure 6. The percentage difference is shown to be 1.9%. However, the simulation data seem to show a minor error where there is a fluctuation of temperature outlet. One of them would involve the multiphase flow setting, and the other might be the precise data for the heat transfer coefficient between the acrylic tube. The comparison temperature outlet for the 5 L/min flow is shown in Figure 7. The percentage of difference is at 4.5%, the highest among the rest of the flow rate. Even though the difference is high, the graphs show a high similarity pattern compared to the other flow rates in the Newtonian region.

Moreover, there is a small spike at the trial count of 110. The difference appears to be more prominent as the temperature reaches wax appearance temperature, leading to phase changes with the deposition of waxes in pipelines. As the pour point temperature of the waxy crude oil used in this study was around 37°C, it can

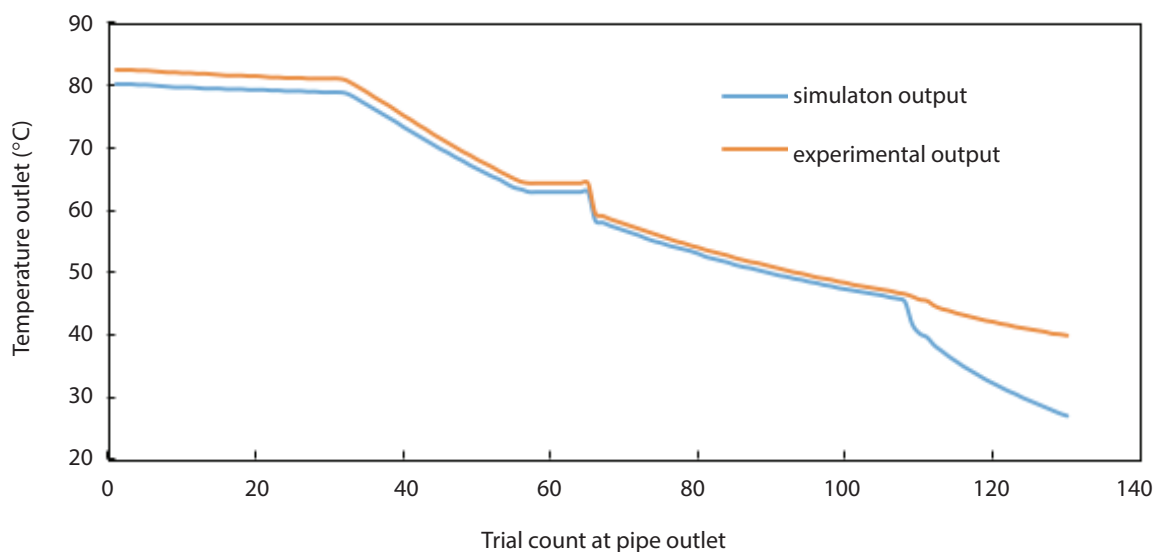


Figure 4 Comparison between experimental and simulated temperature outlet (20 L/min)

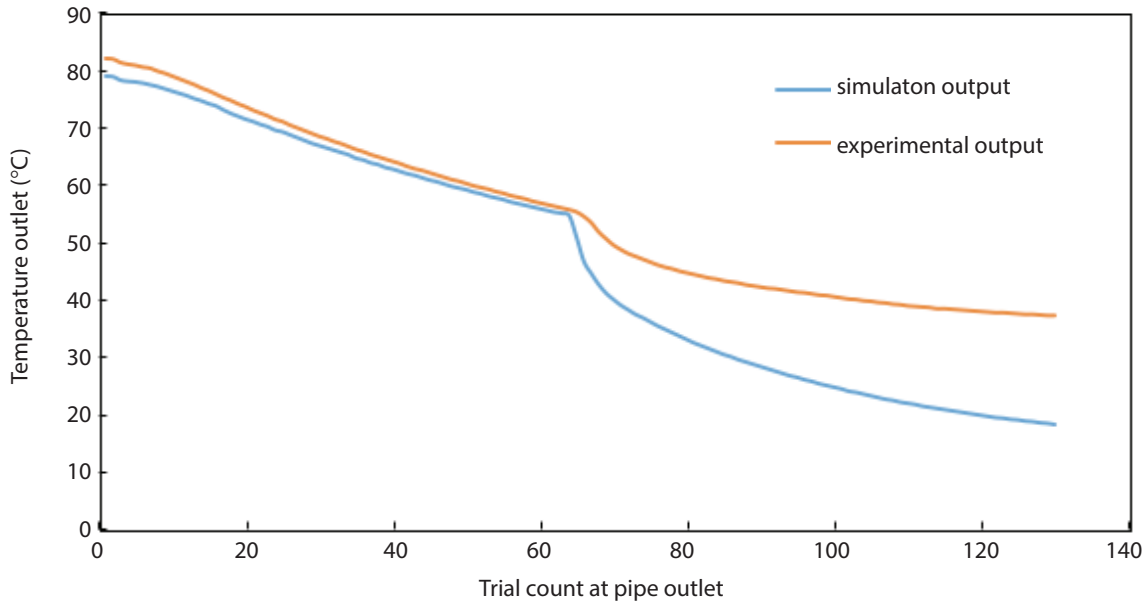


Figure 5 Comparison between experimental and simulated temperature outlet (15 L/min)

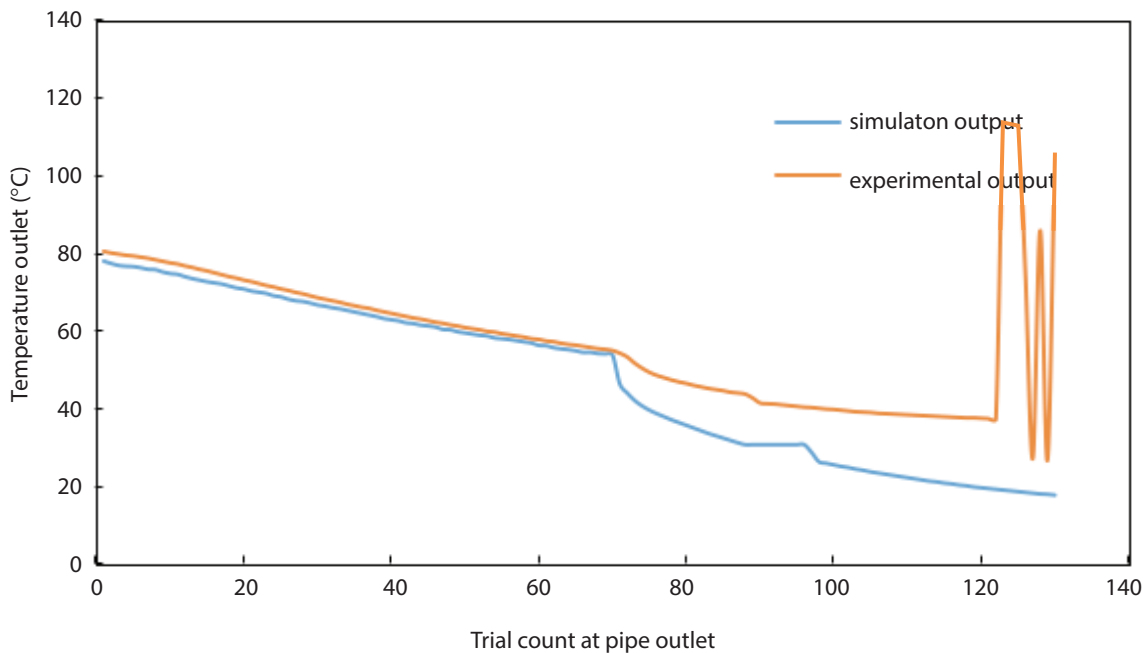


Figure 6 Comparison between experimental and simulated temperature outlet (10 L/min)

be seen that the prediction is not accurate with high spikes below wax appearance temperature with the potential of flow turning to the static condition due to gel formation.

Predictions of flow properties in longer pipes

Waxy crude oil properties in longer pipes were predicted. The same simulation was conducted,

but the set parameter was the length instead. By setting the length as the manipulated variable, the pipe length can be increased to a certain length to determine the temperature outlet of the waxy crude oil. This was intended to replicate the actual waxy crude oil transportation. Hence, this simulation setup would be the first trial benchmark to predict the waxy crude oil in the long-distance pipe. The simulation

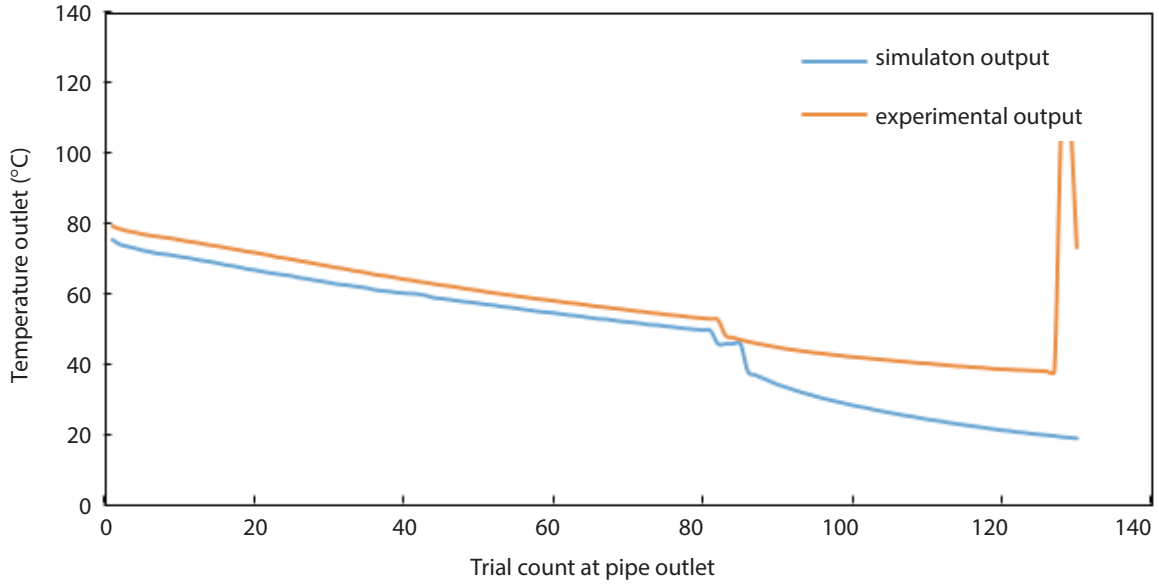
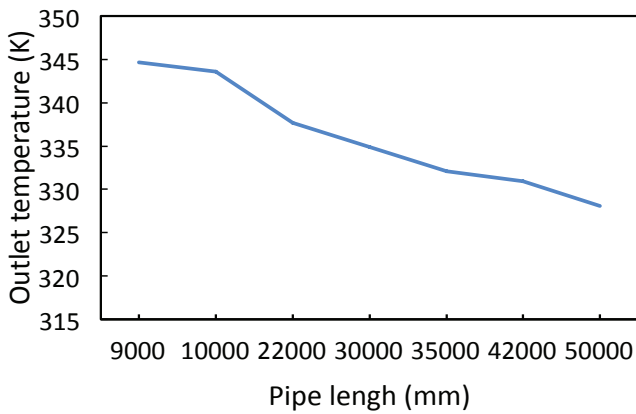
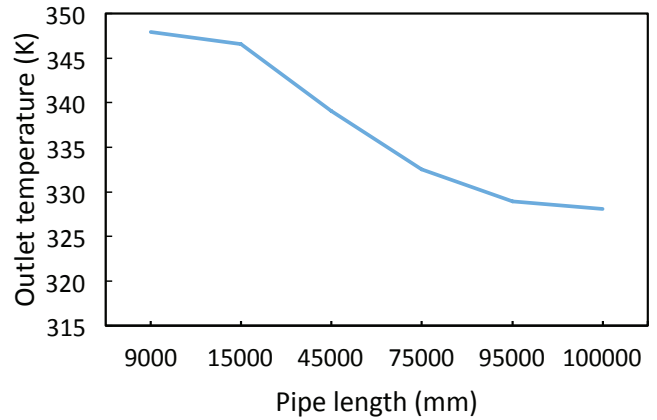


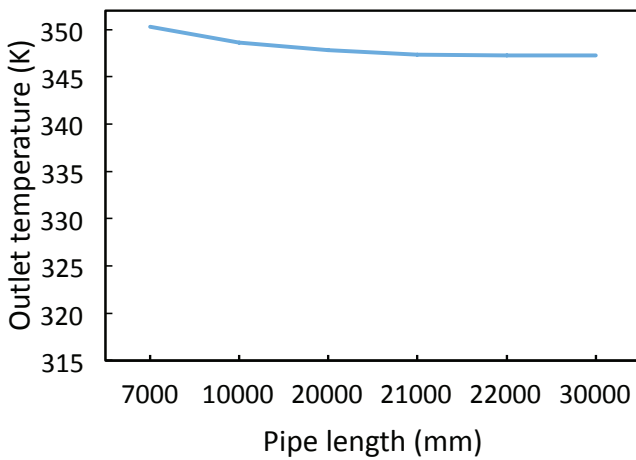
Figure 7 Comparison between experimental and simulated outlet temperature (5 L/min)



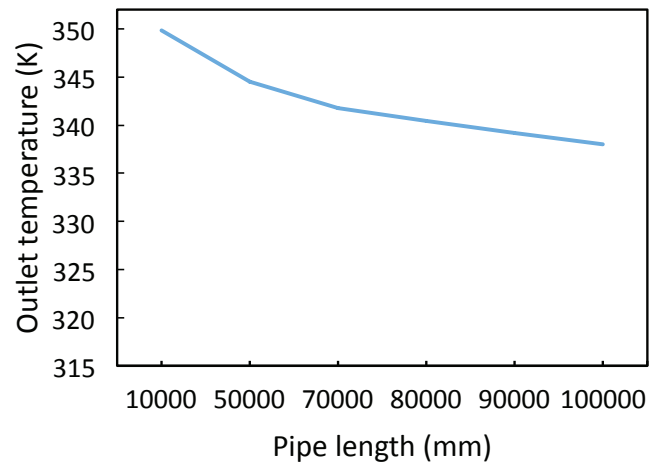
a) 5 L/min



b) 10 L/min



c) 15 L/min



d) 20 L/min

Figure 8 Outlet temperature at the designated pipe length for: a) 5 L/min, b) 10 L/min, c) 15 L/min, and d) 20 L/min

results include the pipe length used in the design of the experiment, the outlet temperature, and the outlet pressure. The outlet temperature is plotted against the length to show the relationship between the responding and the manipulated variable. Figure 8a shows the predicted outlet temperature for the 5 L/min flow rate. The temperature drops until 328.28K (55.25°C) with pipe length of 50 m. While in 10 L/min flow rate (Figure 8b), the longest distance tested was 100 m; however, the outlet temperature was 328.09K (55.09°C.) The pipe length found in the 15 L/min, illustrated in Figure 8c, was 30 m with the outlet temperature of 347.25K (74.25°C). Lastly Figure 8d shows the predicted outlet temperature over a longer pipe for the 20 L/min flow rate. The longest length from the simulation was 100 m with the temperature of 338K (65°C). In general, temperature drop at low temperatures was observed to be smaller as there would be phase changes.

CONCLUSION

A numerical study was carried out to predict the properties of waxy crude oil under dynamic cooling. ANSYS-Fluent parameterisation was used for the analysis. It was observed that the differences between experiment and simulation results are relatively small. The percentage of difference for 20 L/min was 2.6%, 15 L/min has an average of 1.7% percentage difference and 10 L/min has an average of 1.9%. In comparison, the percentage difference for 5 L/min was 4.5%, showing that the simulation model could be used for prediction purposes. However, this is only valid when the crude oil remains in the liquid phase. According to the flow rate and pressure outlet correlation, the flow rate at 20 L/min shows a smooth pressure graph. The longest simulated distance was as long as 100 m with the waxy crude oil outlet temperature of 338K. This demonstrates that the crude oil property has not yet fully reached a solid-state, which is 310K. This prediction would be the spark to use different simulation tools to analyse the waxy crude oil temperature and pressure at a certain distance of the long pipe so that the restart work could be conducted at a much lower cost.

REFERENCES

[1] G.M. de Oliveira & C.O.R. Negrão, "The effect of compressibility on flow start-up of waxy crude oils",

Journal of Non-Newtonian Fluid Mechanics, 220, pp. 137-147, 2015.

- [2] S. Li, Q. Huang, D. Zhao, & Z. Lv, "Relation of heat and mass transfer in wax diffusion in an emulsion of water and waxy crude oil under static condition", *Experimental Thermal and Fluid Science*, 99, pp. 1-12, 2018.
- [3] G. Sun, J. Zhang, C. Ma, & X. Wang, "Start-up flow behavior of pipelines transporting waxy crude oil emulsion", *Journal of Petroleum Science and Engineering*, 147, pp. 746-755, 2016.
- [4] G.T. Chala, C. Chan, & H. Sadig, "Temperature profile and its effects on the location of lower denser substance in waxy crude oil: A numerical study", *Advanced Science Letters*, 24, 11, pp. 8880-8884, 2018.
- [5] A.M. Al-Sabagh, M.N. El-Din, R.E. Morsi, & M.Z. Elsabee, "Styrene-maleic anhydride copolymer esters as flow improvers of waxy crude oil", *Journal of Petroleum Science and Engineering*, 65, 3-4, pp. 139-146, 2009.
- [6] G.B. Tarantino, L.C. Vieira, S.B. Pinheiro, S. Mattedi, L.C.L. Santos, C.A.M. Pires, L.M.N. Gois, & P.C.S. Santos, "Characterization and evaluation of waxy crude oil flow", *Brazilian Journal of Chemical Engineering*, 33, 4, pp. 1063-1071, 2016.
- [7] G.T. Chala, S.A. Sulaiman, & A. Japper-Jaafar, "Flow start-up and transportation of waxy crude oil in pipelines-A review", *Journal of Non-Newtonian Fluid Mechanics*, 251, pp. 69-87, 2018.
- [8] F. Sánchez-Minero, G. Sánchez-Reyna, J. Ancheyta, & G. Marroquin, "Comparison of correlations based on API gravity for predicting viscosity of crude oils", *Fuel*, 138, pp. 193-199, 2014.
- [9] H. Sun, X. Lei, B. Shen, H. Zhang, J. Liu, G. Li, & D. Wu, "Rheological properties and viscosity reduction of South China Sea crude oil", *Journal of Energy Chemistry*, 27, 4, pp. 1198-1207, 2018.
- [10] S.A. Sulaiman, G.T. Chala, & M.Z. Zainur, "Experimental investigation of compressibility of waxy crude oil subjected to static cooling", *Journal of Petroleum Science and Engineering*, 182, 106378, 2019.
- [11] G.T. Chala, A.S. Shaharin, J.-J. Azuraien, W.A. Kamil, & W. Abdullah, "Investigation of convective heat transfer coefficient and initial temperature of waxy crude

- oil on the formation of voids", *International Journal of Automotive and Mechanical Engineering*, 13, 3, pp. 3754-3762, 2016.
- [12] A. Shafquet, I. Ismail, A. Japper-Jaafar, S.A. Sulaiman, & G.T. Chala, "Estimation of gas void formation in statically cooled waxy crude oil using online capacitance measurement", *International Journal of Multiphase Flow*, 75, pp. 257-266, 2015.
- [13] G.T. Chala, S.A. Sulaiman, A. Japper-Jaafar, W. Abdullah, & W.A. Kamil, "Impacts of cooling rates on voids in waxy crude oil under quiescent cooling mode", Paper presented at the Applied Mechanics and Materials, 2015.
- [14] B. Abedi, M.J.P. Miguel, P.R. de Souza Mendes, & R. Mendes, "Startup flow of gelled waxy crude oils in pipelines: The role of volume shrinkage", *Fuel*, 288, pp. 119726, 2021.
- [15] Y. Li, J. Zhao, Y. Liu, H. Dong, & W. Zhao, "The effect of physical properties on the gelation behavior of waxy crude oil during shutdown", *Case Studies in Thermal Engineering*, 21, 100699, 2020.
- [16] H. Li, J. Zhang, C. Song, & G. Sun, "The influence of the heating temperature on the yield stress and pour point of waxy crude oils", *Journal of Petroleum Science and Engineering*, 135, pp. 476-483, 2015.
- [17] A. Japper-Jaafar, P.T. Bhaskoro, L.L. Sean, M.Z. Sariman, & H. Nugroho, "Yield stress measurement of gelled waxy crude oil: Gap size requirement", *Journal of Non-Newtonian Fluid Mechanics*, 218, pp. 71-82, 2015.
- [18] G.T. Chala, S.A. Sulaiman, A. Japper-Jaafar, & W.A.K.W. Abdullah, "Effects of cooling regime on the formation of voids in statically cooled waxy crude oil", *International Journal of Multiphase Flow*, 77, pp. 187-195, 2015.
- [19] L. Kumar, O. Skjæraasen, K. Hald, K. Paso, & J. Sjöblom, "Nonlinear rheology and pressure wave propagation in a thixotropic elasto-viscoplastic fluids, in the context of flow restart", *Journal of Non-Newtonian Fluid Mechanics*, 231, pp. 11-25, 2016.
- [20] P.R. de Souza Mendes, F.S.-M. de Abreu Soares, C.M. Ziglio, & M. Gonçalves, "Startup flow of gelled crudes in pipelines", *Journal of Non-Newtonian Fluid Mechanics*, 179-180, 23-31, 2012.
- [21] G.T. Chala, S.A. Sulaiman, A. Japper-Jaafar, W.A. Kamil Wan Abdullah, & M. M. Mior Mokhtar, "Gas void formation in statically cooled waxy crude oil", *International Journal of Thermal Sciences*, 86, pp. 41-47, 2014.
- [22] T. Firmansyah, M.A. Rakib, A. George, M. Al Musharfy, & M.I. Suleiman, "Transient cooling simulation of atmospheric residue during pipeline shutdowns", *Applied Thermal Engineering*, 106, pp. 22-32, 2016.
- [23] F. Fleyfel, O. Hernandez, R. Sturgis, & W. Meng, "Evaluation of pipeline configurations with active heating for export of waxy crude oil", Paper presented at the SPE Annual Technical Conference and Exhibition, 2004.
- [24] S.K. Elam, I. Tokura, K. Saito, & R.A. Altenkirch, "Thermal conductivity of crude oils", *Experimental Thermal and Fluid Science*, 2, 1, pp. 1-6, 1989.
- [25] Z. Huang, H.S. Lee, M. Senra, & H. Scott Fogler, "A fundamental model of wax deposition in subsea oil pipelines", *AIChE Journal*, 57, 11, pp. 2955-2964, 2011.
- [26] A. Hart, "A review of technologies for transporting heavy crude oil and bitumen via pipelines", *Journal of Petroleum Exploration and Production Technology*, 4, 3, pp. 327-336, 2014.
- [27] M.H. Hassanean, M.E. Awad, H. Marwan, A.A. Bhran, & M. Kaoud, "Studying the rheological properties and the influence of drag reduction on a waxy crude oil in pipeline flow", *Egyptian Journal of Petroleum*, 25, 1, pp. 39-44, 2016.
- [28] S.A. Sulaiman, B.K. Biga, & G.T. Chala, "Injection of non-reacting gas into production pipelines to ease restart pumping of waxy crude oil", *Journal of Petroleum Science and Engineering*, 152, pp. 549-554, 2017.
- [29] J. Zhao, W. Zhao, H. Dong, L. Wei, & Y. Liu, "New approach for the in situ microscopic observation of wax crystals in waxy crude oil during quiescent and dynamic cooling", *ACS Omega*, 5, 20, pp. 11491-11506, 2020.
- [30] G.T. Chala, S.A. Sulaiman, A. Japper-Jaafar, & W.A.K.W. Abdullah, "Study on influence of flow rates on voids in waxy crude oil subjected to dynamic and static cooling", *Journal of Mechanical Engineering and Sciences*, 9, pp. 1586-1594, 2015.

- [31] M. Lin, C. Li, F. Yang, & Y. Ma, "Isothermal structure development of Qinghai waxy crude oil after static and dynamic cooling", *Journal of Petroleum Science and Engineering*, 77, 3, pp. 351-358, 2011.
- [32] F.S. Ribeiro, P.R.S. Mendes, & S.L. Braga, "Obstruction of pipelines due to paraffin deposition during the flow of crude oils", *International Journal of Heat and Mass Transfer*, 40, 18, pp. 4319-4328, 1997.